

DANISH METEOROLOGICAL INSTITUTE

—— SCIENTIFIC REPORT ——

02-06

**A New High Resolution Method for
Processing Radio Occultation Data**

By

**Arne Skov Jensen, Hans-Henrik Benzon
and Martin S. Lohmann**



COPENHAGEN 2002

ISSN Nr. 0905-3263 (printed)
ISSN Nr. 1399-1949 (online)
ISBN-Nr. 87-7478-458-7

A New High Resolution Method for Processing Radio Occultation Data

Arne Skov Jensen, Hans-Henrik Benzon and Martin S. Lohmann

Danish Meteorological Institute, Research and Development Department, Lyngbyvej 100, DK-2100 Copenhagen

Abstract. A new signal processing method for radio occultations is presented. The method is conceptual and computational simple and utilizes the path traversed by the receiving satellite as a synthetic aperture. The large aperture means that a high spatial resolution in the Doppler frequency, and hence in the refractive index, can be achieved. The Doppler frequencies in the received signal are detected through a single Fourier analysis of the entire signal. As a consequence of the spectral approach, multiple frequencies arriving at the receiver at the same instants can be correctly resolved.

Introduction

In general terms, the radio occultation technique is based on the bending of radio waves caused by refractivity index gradients in the atmosphere, [e.g. *Kursinski et al.*, 1997]. In GNSS (Global Navigation Satellite System) radio occultation, the bending is measured as the radio waves traverses the atmosphere from a GNSS satellite to a LEO (Low Earth Orbit) satellite. The atmospheric bending can be retrieved as function of impact parameter from the measured Doppler shifts of the radio signals and the positions and velocities of the satellites. Under the assumption of spherical symmetry, the measured pairs of bending angle and impact parameter can be inverted through the Abel transform to yield the index of refractivity as a function of height [*Fjeldbo et al.*, 1971].

In single ray regions, the computation of bending angles is straightforward as they are unambiguously related to the instantaneous frequency of the received signal. However, radio signals propagating through the lower troposphere may have a very complex structure due to multipath propagation caused by water vapour structures [*Gorbunov et al.*, 1996; *Gorbunov and Gurvich*, 1998]. In these regions of the atmosphere the bending angles cannot be directly derived from the instantaneous frequency of the measured signal in multipath regions. Another drawback of retrieving the bending angle directly from the instantaneous frequency is that the vertical resolution is limited by the size of the Fresnel zone. Thus, there has been much effort

in developing techniques with high vertical resolution, which are capable of correctly retrieving the bending angle profile in multipath regions [Gorbunov, 2001]. So far, four high resolution methods have been proposed for processing of radio occultation signals in multipath regions: (1) back-propagation, [e.g. Gorbunov *et al.*, 1996], (2) radio-optics, [e.g. Lindal *et al.*, 1987; Gorbunov 2001], (3) Fresnel diffraction theory [e.g. Marouf *et al.*, 1986; Mortensen and Høeg, 1998], and (4) canonical transform [Gorbunov, 2001]. All of these methods can be termed radio-holographic since they are based on the analysis of the received complex radio signal.

This paper presents a new high-resolution radio-holographic method. The unique in this theory is that the Doppler shifts are derived directly from the Fourier transform of the entire occultation signal. This is equivalent to consider the path traversed by the receiving satellite during an occultation as one synthetic aperture, which yields a very high vertical resolution. The method effectively resolves multiple frequencies in the received signals.

Description and analysis of the method

Radio occultation signals can in general terms be described as narrow-banded signals with slowly varying amplitude and phase. The instantaneous frequency of the signals is the carrier frequency plus the Doppler shift due to the movement of the satellites and the spatial varying refractive index of the media. In multipath regions, the measured signals are a sum of small-banded signals.

The angular resolution of an antenna with an extend of $\Delta l = vT$, is λ/vT , where λ is the wavelength, v the velocity of the receiver and T the observation time. It is seen that a long observation time T is equivalent to a large antenna and consequently to a high angular resolution. This angular resolution is equivalent to a frequency resolution of $1/T$. Consequently, the optimal observation time is equal to the total duration of an occultation. An uncertainty in frequency is equivalent to an uncertainty in the impact parameter (see Eq. 6). With reasonable values for the satellites movements, the uncertainty in frequency for a measuring time of 100 sec is equivalent to an uncertainty of 2 m for the impact parameter or for the vertical resolution of the refractive index.

As will be shown later, the Doppler frequency is a monotonic function of time during an occultation (excluding scintillation phenomena in the analysis). This is also the case in multipath regions where the Doppler frequency of each path varies monotonically. Hence, a specific Doppler frequency occurs only once during an occultation even though several frequencies may be active at the same instant.

Now, consider an array of narrow banded ideal filters, each with different centre frequencies, pointing in the direction of the incoming electromagnetic field. The filters in this array will respond one by one in time, when the right frequency is present in the signal. Sometimes, in the case of multipath, two or more filters will respond at the same time and sometimes the response will stay for a while at the same filter

depending on how fast the Doppler frequency varies. If the arrival times where each filter responds to the incoming signal and the centre frequency of the filters are recorded, the full information of the Doppler frequency as function of time can be obtained. This ideal filter bank can be realised through a Fourier transform of the entire signal, searching for the time information in the phase (the arrival time in the description above is the phase). This technique will be demonstrated in the following Section.

Fourier transforming the radio occultation signal

Consider the received radio occultation signal, after down-conversion. At high signal to noise ratio this signal has the following form.

$$V(t) = \sum Q_p(t) e^{i\varphi_p(t)}, \quad (1)$$

where φ_p is the phase and Q_p the amplitude of the p^{th} single path.

The numbers of single paths are unknown and irrelevant for the following analysis, and the summation in Eq. 1 is therefore omitted in the following. The Fourier transform sees each single path separately. The Fourier transform of $V(t)$ yields:

$$\hat{V}(\omega, t) = \int_{t-T/2}^{t+T/2} Q_p(t') e^{i(\varphi_p(t') - \omega t')} dt'. \quad (2)$$

If each frequency component in $V(t)$ only occurs once during the observation time of the signal, then the integral above can be evaluated using the method of stationary phase, [Born and Wolf, 1999]. By doing so, the approximated value of the Fourier transformed field yields:

$$\hat{V}(\omega, t) \cong \sqrt{\frac{2\pi}{-\dot{\varphi}_q(t_1)}} Q_q(t_1) \exp i(\varphi_q(t_1) - \omega t_1) \Big|_{\omega=\dot{\varphi}_q(t_1)}, \quad (3)$$

where q refers to the single path that contains the angular frequency, ω and t_1 correspond to the time where the signal contains this angular frequency. Time and frequency are related through the condition $\dot{\varphi}_q(t_1) = \omega$, that maps t_1 into the ω space.

In Eq. 3, only phase terms up to second order are included. The validity of this approximation relies on the assumption that the amplitude and the higher order phase terms are slowly varying compared to the time scale of the second order term, $\tau = \sqrt{2\pi/|\ddot{\varphi}_q|}$. This constrain will be verified later.

The arrival times corresponding to the different frequencies in the signal can now be found by differentiating the phase, u , of the Fourier transform given by Eq. 3 with respect to frequency:

$$\frac{du}{d\omega} = \frac{d}{d\omega} (\varphi_q(t_1) - \omega t_1) = \frac{d\varphi_q}{dt_1} \frac{dt_1}{d\omega} - \omega \frac{dt_1}{d\omega} - t_1 = -t_1, \quad (4)$$

or

$$\left(\omega, -\frac{d\varphi}{d\omega}\right) = (\omega(t), t).$$

Hence, the arrival times of the frequency components in the Fourier spectrum is simply given as the derivatives of the phases of conjugated Fourier components.

The Fourier technique is very robust and insensitive to signal fading and fallouts that may occur during an occultation. Due to the long measuring time the frequency resolution and thereby the vertical resolution of the refractive index is very high compared to the Fresnel zone limitation. The impact of white noise in this method does not cause other problem than encountered in usual spectrum analysis with a sliding time window.

Verification of assumptions

Eqs. 3 and 4 were derived assuming that the amplitude and the higher order phase terms are slowly varying compared to the time scale of the second order phase term. Furthermore, it was assumed that the Doppler frequency is monotonic function of time for each single path. These assumptions will be verified in the following.

The phase of an occultation is, in geometrical optical terms, the optical path between the transmitter and receiver. For a configuration with a GPS satellite as transmitter and a low orbit satellite (LEO) as receiver, the phase can be written in several forms [Melbourne *et al.*, 1994], but for this analysis the following form is appropriate:

$$\varphi = k \int_{r_0}^{r_L} \frac{\sqrt{n^2 r^2 - a^2}}{r} dr + k \int_{r_0}^{r_G} \frac{\sqrt{n^2 r^2 - a^2}}{r} dr + ka\theta, \quad (5)$$

where index G and L are referring to the GPS and the LEO satellite, respectively. r is distance from the Earth, θ the angle between the satellites, and k is the wave number. The time derivative of the phase, the Doppler frequency, yields:

$$\omega(t) = \dot{\varphi}(t) = k\dot{r}_G \cos(\psi_G) + k\dot{r}_L \cos(\psi_L) + ka\dot{\theta}, \quad (6)$$

where $\dot{\theta} = \Omega$ (assumed to be a constant).

If the radial velocities of the satellites are very small or zero the Doppler frequency is proportional to the impact parameter. Due to this proportionality, the frequency of each single path will vary monotonically with time. The second derivative of the phase, which gives the time scale, yields:

$$\ddot{\varphi} \cong k\Omega\dot{a} = k\Omega^2 \left(\frac{d\theta}{da}\right)^{-1}, \quad (7)$$

where $d\theta/da$ is the defocusing factor.

The amplitude Q can be expressed as [Leroy, 2001]:

$$Q(t) = \left[\frac{P_G}{2\pi} \frac{a}{r_G r_L \sin(\theta) r_G \cos(\psi_G) r_L \cos(\psi_L)} \frac{d\theta}{da} \right]^{\frac{1}{2}}, \quad (8)$$

where ψ is the angle between the radius and the ray path, a is the impact parameter, P is the transmitted signal power, and θ the angle between the satellites.

Inserting Eqs. 7 and 8 into Eq. 3 yields the Fourier transform of the occultation signal:

$$\hat{V}(\omega, t) \cong \sqrt{\frac{2\pi i}{-\dot{\phi}(t_1)}} Q(t_1) e^{i(\phi(t_1) - \omega t_1)} \Big|_{\omega = \dot{\phi}(t_1)} = \left(\frac{a P_G}{r_G r_L \sin(\theta) r_G \cos(\psi_G) r_L \cos(\psi_L)} \right)^{\frac{1}{2}} e^{i(\phi(t_1) - \omega t_1)} \Big|_{\omega = \dot{\phi}(t_1)}. \quad (9)$$

In vacuum the time scale associated with ϕ is of the order 0.2-0.3 sec. In the atmosphere the time scale is approximately the same or longer if gradients are present. The defocusing factor, $d\theta/da$, gives the main time scale for the amplitude variations (see Eq. 8), so in this respect the assumption concerning the time variation of the amplitude is 'self-fulfilled' due to the physics of the occultation. The higher order phase terms (from third order and on) depend on angular velocity Ω ($\Omega \approx 10^{-3} \text{ rad/sec}$) in powers of the order, thus it seems to be safe to assume that these terms are decaying very fast.

Results from a forward propagated simulated occultation signal

The data used for this simulation is a wave propagation in the atmosphere based on the solution of the Helmholtz wave equation. This approach applies a full wave, forward scatter model that is capable of predicting propagation for an arbitrary atmospheric refractivity. The primary limitations of this technique are that it neglects the backscattered field, and that accurate calculations are restricted to near-horizontal propagation directions.

The wave propagator is used on a meteorological weather predicting analysts field (ECHAM GRIB file no. 62, Feb. 2, 1997). An occultation has been selected so the wave propagating from the GPS satellite to the LEO satellite will enter areas in the neutral atmosphere where strong variations in the index of refraction occur. The simulated amplitude and phase signals for the L1 wave, are calculated for the position of the LEO satellite. The resulting signal consists of the simulated amplitude and the excess phase i.e. the phase from the neutral atmosphere subtracted from the real phase. This reduces the necessary sampling rate. The sampling rate for the simulation used here is 58 Hz.

Now, before the signal is processed, the 'original' signal has to be reconstructed, at least to a point where the bandwidth of the reconstructed signal is equal to the original

signal. This is done by a re-sampling (interpolation) of the simulated signal, and by adding the phase from the neutral atmosphere. The restored complex signal has a bandwidth of approx. 500 Hz.

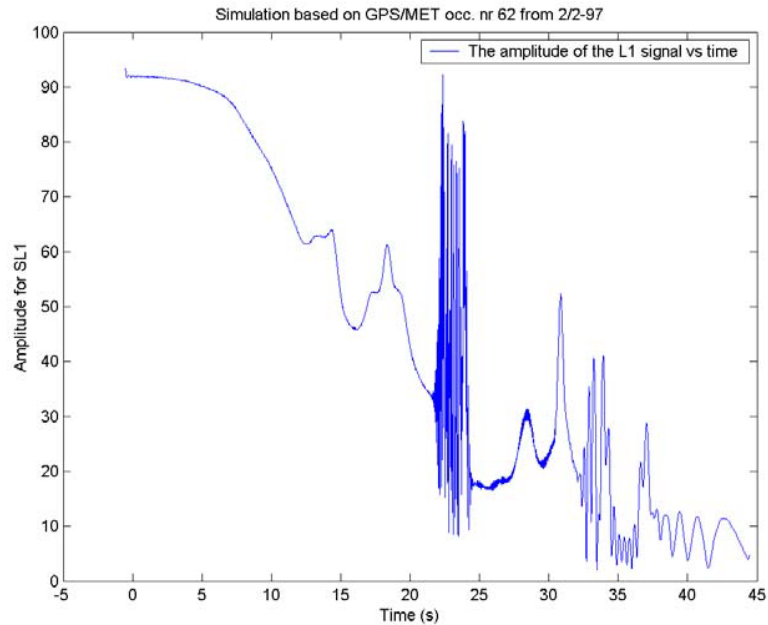


Fig 1. The amplitude of an occultation signal.

In Fig.1 the amplitude of the occultation signal is shown. It is seen that signs of strong multipath (significant variations in the amplitude due interference) are present around 23, 33 and 36 sec. Other extremes in the amplitude can be associated with variations in the defocusing factor.

The results from a FFT of the restored signal are shown in Fig. 2. Within the bandwidth of the signal the FFT spectrum is flat as predicted in Eq. 9.

The phase of the FFT is differentiated with respect to the frequency giving the time (see Eq. 4). This is shown in Fig. 3 and 4 in blue colour. Fig. 4 shows a magnification of Fig. 3 in order to be able to discern the details in the plot. For comparison, the Doppler frequency (the time derivative of the measured phase) is mapped versus time in a red colour. It is seen that the two curves are overlapping by near areas where multipaths are occurring. The points in Fig. 3 and 4 are not connected, instead one views clustering of points.

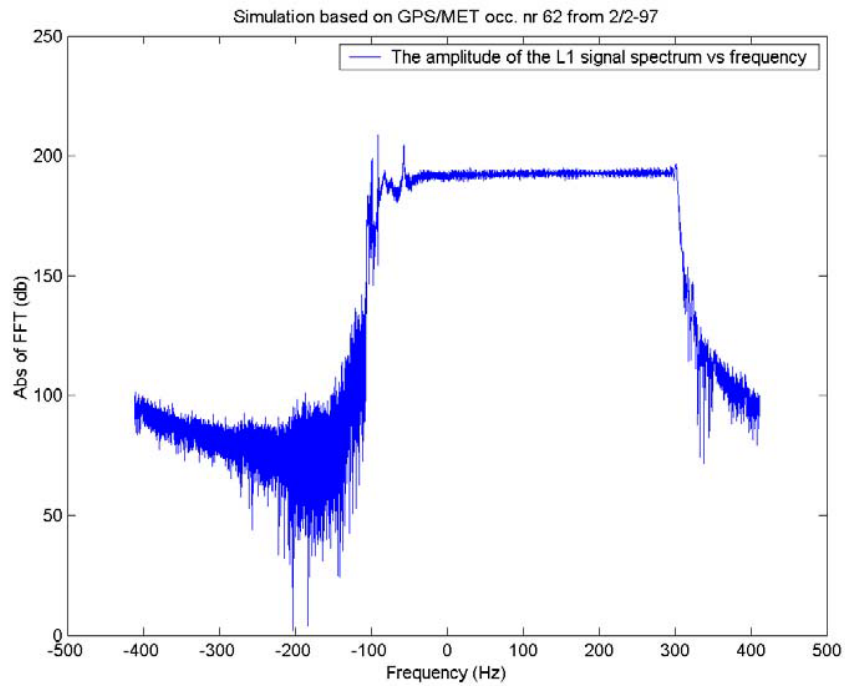


Fig 2. The FFT amplitude spectrum of the signal.

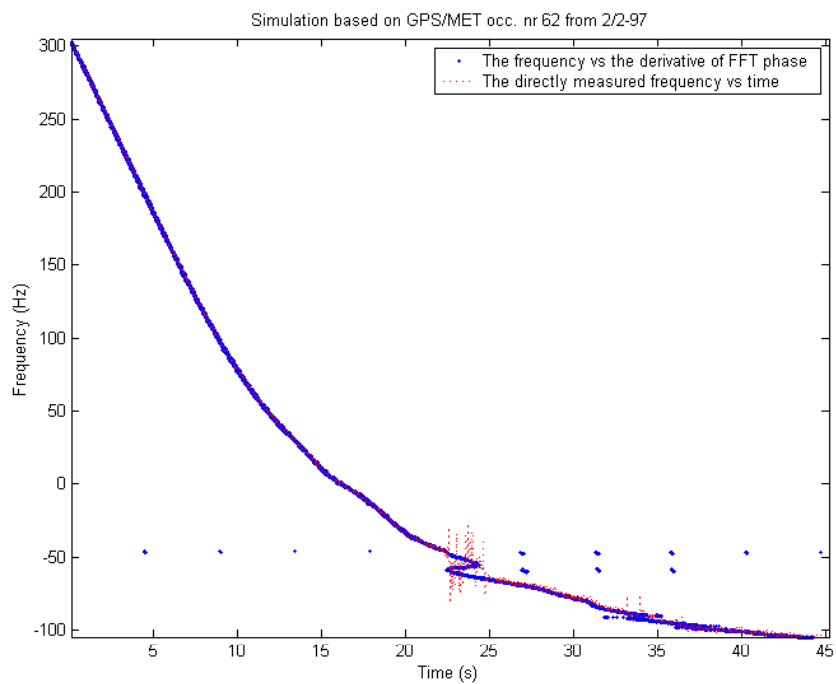


Fig 3. The derivative of the FFT-phase with respect to the frequency displayed in blue colour. The red curve is Doppler frequency vs. time.

The Doppler frequency vs. time (the red curve) shows a very irregular behaviour at the first multipath area around the abscissa 23 sec. in fig 3& 4. This is expected, since pure phase detection will not reveal multipath. The derivative of the FFT phase shows clearly the expected form of multipath at least in three places in Fig. 4 located at 23, 33 and 36 sec.

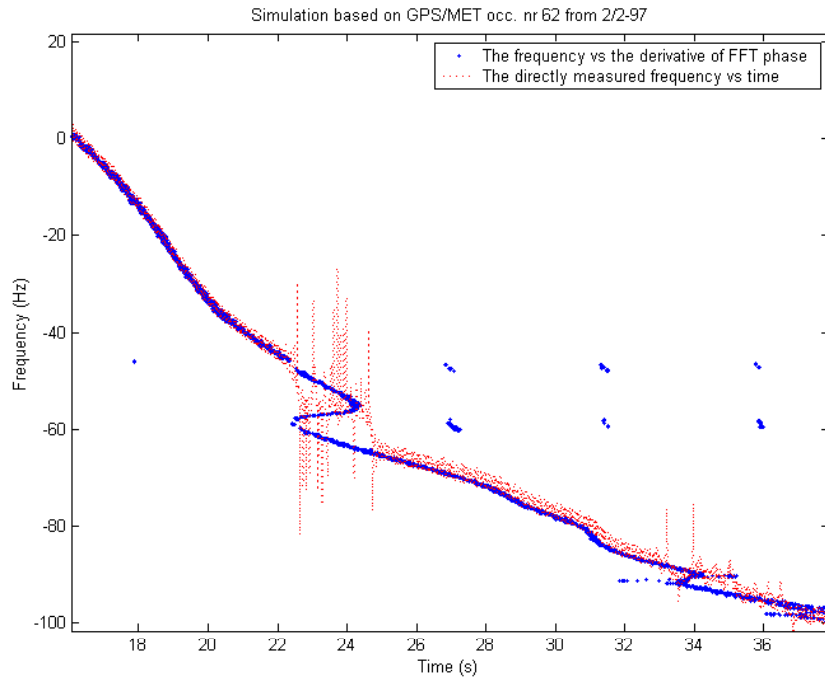


Fig 4. The figure shows a magnification of Fig. 3.

In the spectrum of Fig. 2, a peak at -50 Hz and a lot of scattered points in the graph of the derivative of the FFT (Fig. 3 & 4) is seen. The peak should not be present according to Eq. 9 and the scattered points seem unphysical. These effects can be caused by several factors: a) If the scattered points are not caused by errors in the generation of the occultation signal, then the used sampling rate of 58 Hz has not been sufficient. As seen from Fig. 3 the adequate sampling rate should have been at least 250 Hz. b) The wave propagator exhibits problems in generating a correct signal in multipath situations. c) The observed effects are real and caused by strong fluctuations generated in the signals.

At this stage it has not been possible to investigate the mentioned error sources, but the general results of the signal processing seem to coincide with the developed theory.

Conclusion

A new method for processing radio occultation signals has been presented. The results of the simulated occultation data seem to confirm the theoretical results. The amplitude spectrum of the occultation signal is close to a straight line, reflecting that the defocusing factor in the signal amplitude is cancelled out by the Fourier transform. Deviations from this could be used to detect scintillations in the atmosphere and also be useful in absorption measurements done with different carrier frequencies.

A comparison with other methods has not been the aim here, but it will be considered in future investigations. The high spatial resolution, the possibility for detections of scintillations through deviations from the ideal spectrum and the simplicity both conceptual and computational seem to be very promising for the practical application of the method.

Acknowledgement

This work was supported by the European Space Agency, ESTEC contract no. 14809/00/NL/MM.

References

- Born, M. and E. Wolf, Principles of Optics, pp 888-890, Cambridge University Press, 1999.
- Fjeldbo, G., A. J. Kliore, and Eshlermann. The neutral atmosphere of Venus Studied with the Mariner V radio occultation experiments, *Astron. J.*, 76(2), 123-140, 1971.
- Gorbunov, M. E., S. V. Sokolovskiy, and L. Bengtson, Advanced algorithms of inversion of GPS/MET satellite data and their application to reconstruction of temperature and humidity *Tech. Rep Report No. 211*, Max Planck Institute for Meteorology, Hamburg, 1996.
- Gorbunov, M. E. and A. S. Gurvich, Microlab-1 experiment: Multipath effects in the lower troposphere. *J. Geophys. Res.*, 103(D12), 13,819-826, 1998.
- Gorbunov, M. E., Radioholographic methods for processing radio occultation data in multipath regions, *Scientific Report 01-02*, Danish Meteorological Institute, Copenhagen, 2001.
- Kursinski, E. R., G. A. Hajj, J. T. Schofield, and R. P. Linfield, Observing Earth's Atmosphere with Radio Occultation Measurements using Global Positioning System. *J. Geophys. Res.*, 102,(D19), 23,429-465, 1997.
- Leroy, S. S., Amplitude of an occultation signal in three dimensions, Submitted to *Radio Science*, 2001.
- Lindal, G. F., J. R. Lyons, D. N. Sweetnam, V. R. Eshleman, D. P. Hinson, and G. L. Tyler, The atmosphere of Uranus: Results of radio occultation measurements with Voyager 2, *J. Geophys. Res.*, 92(A13), 14,987-001, 1987.
- Meincke, M. D., Inversion methods for atmospheric profiling with GPS occultations. *Scientific Report 99-11*, Danish Meteorological Institute, Copenhagen, 1999.
- Melbourne, W. G., E. S. Davis, C. B. Duncan, G. A. Hajj, K. R. Hardy, E. R. Kursinski, T. K. Meehan, L. E. Young, T. P. Younck, The application of GPS limb sounding and global change monitoring. *JPL publication 94-18*, JPL, Pasadena, CA, USA, 1994.
- Mortensen, M. D. and P. Høeg, Inversion of GPS occultation measurements using Fresnel diffraction theory. *Geophys Res. Letters*, 25(13), 2446-2449, 1998.

Arne Skov Jensen, asj@dmi.dk, Hans-Henrik Benzon, hjb@dmi.dk and Martin S. Lohmann, lmsl@dmi.dk

Danish Meteorological Institute, Research and Development Department, Lyngbyvej 100, DK-2100 Copenhagen

DANISH METEOROLOGICAL INSTITUTE

Scientific Reports

Scientific reports from the Danish Meteorological Institute cover a variety of geophysical fields, i.e. meteorology (including climatology), oceanography, subjects on air and sea pollution, geomagnetism, solar-terrestrial physics, and physics of the middle and upper atmosphere.

Reports in the series within the last five years:

No. 97-1

E. Friis Christensen og C. Skøtt: Contributions from the International Science Team. The Ørsted Mission - a pre-launch compendium

No. 97-2

Alix Rasmussen, Sissi Kiilsholm, Jens Havskov Sørensen, Ib Steen Mikkelsen: Analysis of tropospheric ozone measurements in Greenland: Contract No. EV5V-CT93-0318 (DG 12 DTEE); DMI's contribution to CEC Final Report Arctic Tropospheric Ozone Chemistry ARCTOC

No. 97-3

Peter Thejll: A search for effects of external events on terrestrial atmospheric pressure: cosmic rays

No. 97-4

Peter Thejll: A search for effects of external events on terrestrial atmospheric pressure: sector boundary crossings

No. 97-5

Knud Lassen: Twentieth century retreat of sea-ice in the Greenland Sea

No. 98-1

Niels Woetman Nielsen, Bjarne Amstrup, Jess U. Jørgensen: HIRLAM 2.5 parallel tests at DMI: sensitivity to type of schemes for turbulence, moist processes and advection

No. 98-2

Per Høeg, Georg Bergeton Larsen, Hans-Henrik Benzon, Stig Syndergaard, Mette Dahl Mortensen: The GPSOS project
Algorithm functional design and analysis of ionosphere, stratosphere and troposphere observations

No. 98-3

Mette Dahl Mortensen, Per Høeg: Satellite atmosphere profiling retrieval in a nonlinear troposphere
Previously entitled: Limitations induced by Multipath

No. 98-4

Mette Dahl Mortensen, Per Høeg: Resolution properties in atmospheric profiling with GPS

No. 98-5

R.S. Gill and M. K. Rosengren: Evaluation of the Radarsat imagery for the operational mapping of sea ice around Greenland in 1997

No. 98-6

R.S. Gill, H.H. Valeur, P. Nielsen and K.Q. Hansen: Using ERS SAR images in the operational mapping of sea ice in the Greenland waters: final report for ESA-ESRIN's: pilot projekt no. PP2.PP2.DK2 and 2nd announcement of opportunity for the exploitation of ERS data projekt No. AO2..DK 102

No. 98-7

Per Høeg et al.: GPS Atmosphere profiling methods and error assessments

No. 98-8

H. Svensmark, N. Woetmann Nielsen and A.M. Sempreviva: Large scale soft and hard turbulent states of the atmosphere

No. 98-9

Philippe Lopez, Eigil Kaas and Annette Guldborg: The full particle-in-cell advection scheme in spherical geometry

No. 98-10

H. Svensmark: Influence of cosmic rays on earth's climate

No. 98-11

Peter Thejll and Henrik Svensmark: Notes on the method of normalized multivariate regression

No. 98-12

K. Lassen: Extent of sea ice in the Greenland Sea 1877-1997: an extension of DMI Scientific Report 97-5

No. 98-13

Niels Larsen, Alberto Adriani and Guido DiDonfrancesco: Microphysical analysis of polar stratospheric clouds observed by lidar at McMurdo, Antarctica

No.98-14

Mette Dahl Mortensen: The back-propagation method for inversion of radio occultation data

No. 98-15

Xiang-Yu Huang: Variational analysis using spatial filters

No. 99-1

Henrik Feddersen: Project on prediction of climate variations on seasonal to interannual timescales (PROVOST) EU contract ENV4-CT95-0109: DMI contribution to the final report: Statistical analysis and post-processing of uncoupled PROVOST simulations

No. 99-2

Wilhelm May: A time-slice experiment with the ECHAM4 A-GCM at high resolution: the experimental design and the assessment of climate change as compared to a greenhouse gas experiment with ECHAM4/OPYC at low resolution

No. 99-3

Niels Larsen et al.: European stratospheric monitoring stations in the Arctic II: CEC Environment and Climate Programme Contract ENV4-CT95-0136. DMI Contributions to the project

No. 99-4

Alexander Baklanov: Parameterisation of the deposition processes and radioactive decay: a review and some preliminary results with the DERMA model

No. 99-5

Mette Dahl Mortensen: Non-linear high resolution inversion of radio occultation data

No. 99-6

Stig Syndergaard: Retrieval analysis and methodologies in atmospheric limb sounding using the GNSS radio occultation technique

No. 99-7

Jun She, Jacob Woge Nielsen: Operational wave forecasts over the Baltic and North Sea

No. 99-8

Henrik Feddersen: Monthly temperature forecasts for Denmark - statistical or dynamical?

No. 99-9

P. Thejll, K. Lassen: Solar forcing of the Northern hemisphere air temperature: new data

No. 99-10

Torben Stockflet Jørgensen, Aksel Walløe Hansen: Comment on "Variation of cosmic ray flux and global coverage - a missing link in solar-climate relationships" by Henrik Svensmark and Eigil Friis-Christensen

No. 99-11

Mette Dahl Meincke: Inversion methods for atmospheric profiling with GPS occultations

No. 99-12

Hans-Henrik Benzon; Laust Olsen; Per Høeg: Simulations of current density measurements with a Faraday Current Meter and a magnetometer

No. 00-01

Per Høeg; G. Leppelmeier: ACE - Atmosphere Climate Experiment

No. 00-02

Per Høeg: FACE-IT: Field-Aligned Current Experiment in the Ionosphere and Thermosphere

No. 00-03

Allan Gross: Surface ozone and tropospheric chemistry with applications to regional air quality modeling. PhD thesis

No. 00-04

Henrik Vedel: Conversion of WGS84 geometric heights to NWP model HIRLAM geopotential heights

No. 00-05

Jérôme Chenevez: Advection experiments with DMI-Hirlam-Tracer

No. 00-06

Niels Larsen: Polar stratospheric clouds microphysical and optical models

No. 00-07

Alix Rasmussen: "Uncertainty of meteorological parameters from DMI-HIRLAM"

No. 00-08

A.L. Morozova: Solar activity and Earth's weather. Effect of the forced atmospheric transparency changes on the troposphere temperature profile studied with atmospheric models

No. 00-09

Niels Larsen, Bjørn M. Knudsen, Michael Gauss, Giovanni Pitari: Effects from high-speed civil traffic aircraft emissions on polar stratospheric clouds

No. 00-10

Søren Andersen: Evaluation of SSM/I sea ice algorithms for use in the SAF on ocean and sea ice, July 2000

No. 00-11

Claus Petersen, Niels Woetmann Nielsen: Diagnosis of visibility in DMI-HIRLAM

No. 00-12

Erik Buch: A monograph on the physical oceanography of the Greenland waters

No. 00-13

M. Steffensen: Stability indices as indicators of lightning and thunder

No. 00-14

Bjarne Amstrup, Kristian S. Mogensen, Xiang-Yu Huang: Use of GPS observations in an optimum interpolation based data assimilation system

No. 00-15

Mads Hvid Nielsen: Dynamisk beskrivelse og hydrografisk klassifikation af den jyske kyststrøm

No. 00-16

Kristian S. Mogensen, Jess U. Jørgensen, Bjarne Amstrup, Xiaohua Yang and Xiang-Yu Huang: Towards an operational implementation of HIRLAM 3D-VAR at DMI

No. 00-17

Sattler, Kai; Huang, Xiang-Yu: Structure function characteristics for 2 meter temperature and relative humidity in different horizontal resolutions

No. 00-18

Niels Larsen, Ib Steen Mikkelsen, Bjørn M. Knudsen m.fl.: In-situ analysis of aerosols and gases in the polar stratosphere. A contribution to THESEO. Environment and climate research programme. Contract no. ENV4-CT97-0523. Final report

No. 00-19

Amstrup, Bjarne: EUCOS observing system experiments with the DMI HIRLAM optimum interpolation analysis and forecasting system

No. 01-01

V.O. Papitashvili, L.I. Gromova, V.A. Popov and O. Rasmussen: Northern polar cap magnetic activity index PCN: Effective area, universal time, seasonal, and solar cycle variations

No. 01-02

M.E. Gorbunov: Radiological methods for processing radio occultation data in multipath regions

No. 01-03

Niels Woetmann Nielsen; Claus Petersen: Calculation of wind gusts in DMI-HIRLAM

No. 01-04

Vladimir Penenko; Alexander Baklanov: Methods of sensitivity theory and inverse modeling for estimation of source parameter and risk/vulnerability areas

No. 01-05

Sergej Zilitinkevich; Alexander Baklanov; Jutta Rost; Ann-Sofi Smedman, Vasilij Lykosov and Pierluigi Calanca: Diagnostic and prognostic equations for the depth of the stably stratified Ekman boundary layer

No. 01-06

Bjarne Amstrup: Impact of ATOVS AMSU-A radiance data in the DMI-HIRLAM 3D-Var analysis and forecasting system

No. 01-07

Sergej Zilitinkevich; Alexander Baklanov: Calculation of the height of stable boundary layers in operational models

No. 01-08

Vibeke Huess: Sea level variations in the North Sea – from tide gauges, altimetry and modelling

No. 01-09

Alexander Baklanov and Alexander Mahura: Atmospheric transport pathways, vulnerability and possible accidental consequences from nuclear risk sites: methodology for probabilistic atmospheric studies

No. 02-01

Bent Hansen Sass and Claus Petersen: Short range atmospheric forecasts using a nudging procedure to combine analyses of cloud and precipitation with a numerical forecast model

No. 02-02

Erik Buch: Present oceanographic conditions in Greenland waters

No. 02-03

Bjørn M. Knudsen, Signe B. Andersen and Allan Gross: Contribution of the Danish Meteorological Institute to the final report of SAMMOA. CEC contract EVK2-1999-00315: Spring-to.-autumn measurements and modelling of ozone and active species

No. 02-04

Nicolai Kliem: Numerical ocean and sea ice modeling: the area around Cape Farewell (Ph.D. thesis)

No. 02-05

Niels Woetmann Nielsen: The structure and dynamics of the atmospheric boundary layer

No. 02-06

Arne Skov Jensen, Hans-Henrik Benzon and Martin S. Lohmann: A new high resolution method for processing radio occultation data